

12 Boötis: a test bed for extra-mixing processes in stars

Andrea Miglio¹, Josefina Montalbán¹ and Carla Maceroni²

¹*Institut d’Astrophysique et de Géophysique de l’Université de Liège, Allée du 6 Août, 17 B-4000 Liège, Belgium*

²*INAF-Osservatorio di Roma, via Frascati-33, Monteporzio Catone (RM), Italy*

Accepted 1988 December 15. Received 1988 December 14; in original form 1988 October 11

ABSTRACT

12 Boötis is a spectroscopic binary whose visual orbit has been resolved by interferometry. Though the physical parameters of the system have been determined with an excellent precision, the theoretical modelling of the components is still uncertain. We study the capability of solar-like oscillations to distinguish between calibrated models of the system obtained by including in the stellar modelling different mixing processes. We consider different scenarios for the chemical transport processes: classical overshooting, microscopic diffusion and turbulent mixing. For each of them we calibrate the stellar models of 12 Boo A and B by fitting the available observational constraints by means of a Levenberg-Marquardt minimization algorithm, and finally, we analyze the asteroseismic properties of different calibrated models. Several solutions with 12 Boo A in (or close to) post-main sequence and 12 Boo B on main sequence are found by assuming a thickness of the overshooting layer between 0.06 and 0.23 the pressure scale height. Solutions with both components on the main sequence can be found only by assuming an overshoot larger in the primary than in the secondary, or a more efficient central mixing for 12 Boo A than for 12 Boo B. We show that the detection of solar-like oscillations expected in these stars would allow to distinguish between different scenarios and provide therefore an estimation of the overshooting parameters and of the properties of extra-mixing processes.

Key words: stars: binaries – stars: oscillations – stars: interiors – stars: fundamental parameters – stars: individual: 12 Boo

1 INTRODUCTION

In standard stellar modelling convection is described by means of a local theory such as the Mixing Length Theory (Böhm-Vitense 1958), and the extension of the convective regions is determined by the classical Schwarzschild criterion ($\nabla_{\text{rad}} = \nabla_{\text{ad}}$). This is one of the well known shortcomings of stellar structure and evolution theory. For intermediate and high mass stars, where a convective core is developed, the mass of this central mixed region plays a fundamental role in determining the lifetime and the luminosity of the main sequence phase, and affects other relevant aspects such as the s-process nucleosynthesis on the asymptotic giant branch (Ventura & D’Antona 2005), the chemical evolution of the interstellar medium, and the size and composition of white dwarfs (see, e.g. Chiosi 1998).

We mean here by overshooting or extra-mixed region the mixing of material beyond the formal boundary of convection region set by the Schwarzschild criterion. There is quite a large number of observational evidences indicating that this phenomenon of overshooting exists. For instance, comparisons between observations (binaries and open clusters, Andersen et al. 1990; Ribas et al. 2000) and theoretic-

cal models indicate that stars have larger convective cores than predicted by theory. Moreover, numerical simulations and laboratory experiments suggest the overshoot of convective elements in the adjacent stable regions. A great effort has been done during the last 30 years to describe turbulent convection in stellar interiors modelling, however, given the difficulty in estimating the rate of dissipation of turbulent kinetic energy, it is still not possible to predict the thickness of the extra-mixed region from first principles. Therefore, the thickness of the overshooted region (Λ_{OV}) is usually parameterized in terms of the local pressure scale height H_p ($\Lambda_{\text{OV}} = \alpha_{\text{OV}} H_p$). The value of this parameter has been estimated by fitting theoretical isochrones to the observed color-magnitude diagrams of open clusters, and by modelling double-lined eclipsing binaries with well determined masses and radii (see e.g. Ribas et al. 2000). These calibrations also indicate that the exact value of the overshoot parameter might depend on the stellar mass: values of the order of 0-0.1 are required for masses between 1.1 and 1.5 M_{\odot} , and values from 0.2 to 0.5 are needed in the 1.6 to 9 M_{\odot} interval (see Ribas et al. 2000). Moreover, as noticed in VandenBerg & Stetson (2004) and VandenBerg et al. (2006), the overshooting parameter has

probably a steep dependence on mass in the range $1.3 \lesssim M/M_{\odot} \lesssim 1.55$.

Not only the exact amount of overshooting and its dependence on the stellar mass, but also the physical processes responsible for extra-mixing, are still matter of a lively debate (Maeder & Zahn 1998; Young & Arnett 2005; Popielski & Dziembowski 2005).

In this context the binary system 12 Boötis represents a valuable observational test of stellar modelling. Recent interferometric measurements allowed Boden et al. (2005) to determine the masses of the components of this double-lined spectroscopic binary with a precision of about 0.3%. The masses of the components are very similar (mass ratio $q \sim 0.97$), but their luminosities are quite different. A preliminary determination of stellar parameters by comparison with theoretical isochrones (see Boden et al. 2005), suggested that secondary component is still in the central-hydrogen burning phase, while the primary is more evolved and burning hydrogen in a shell. Given the lifetime of the sub-giant phase derived from theoretical models, this solution is quite unlikely (Andersen et al. 1990). Furthermore, as shown by Boden et al. (2005), the evolutionary state of the fitted models is highly dependent on the model details (and in particular on the amount of core overshooting) and needs further investigation. The masses of 12 Boo components (1.416 and 1.372 M_{\odot}) are in fact in the transition region, where the thickness of the “overshooting” layer seems to depend on the stellar mass, metallicity and evolutionary stage (VandenBerg et al. 2006).

Even if the masses are very precisely known, and both the components have the same age and initial chemical composition, there is a large number of possible parameter sets able to fit the “classical” observables. In this paper we present different scenarios based on different theoretical prescriptions for extra-mixing processes, which provide stellar parameters compatibles with observational constraints, but with different evolutionary state and internal structure. The classical observables do not allow to distinguish between different solutions, and hence additional and independent observational constraints are needed. In this paper we propose solar-like oscillations as additional observational constraints. Fortunately, the components of 12 Boo are located in a region where solar-like oscillations are expected to be excited (see e.g. Kjeldsen & Bedding 1995; Houdek et al. 1999 and Samadi et al. 2005).

Solar-like oscillations have been observed in several single stars (e.g. η Boötis, and μ Arae, Kjeldsen & Bedding 1995; Bouchy et al. 2005, respectively) and binary systems (Procyon, Martić et al. 2004) as well as in both components of the visual binary system α Centauri (Bouchy & Carrier 2002; Carrier & Bourban 2003; Bedding et al. 2004; Kjeldsen et al. 2005). In the latter, as shown by Miglio & Montalbán (2005), the combination of asteroseismic and precise “classical” constraints (masses, radii, luminosities ...) significantly improves the determination of the system fundamental parameters. While the study of α Centauri provides a test of our knowledge of stellar structure in conditions that are slightly different from the Sun, a detailed investigation of 12 Boötis will be a relevant step in understanding the structure of the central regions for this particular area in the Hertzsprung-Russell diagram

(HRD) where the “transition” from radiative to convective core models takes place.

In Sect. 2 we summarize the observational knowledge about 12 Boo, and we describe the constraints will be used in the calibration process. The latter is described in Sec. 3. Among the free parameters, the most important is the extension of the overshooting region. We will also analyse possible solutions by taking into account different physical processes able to change the thickness and features of the extra mixed region. In Sec. 4 we study how the differences in the stellar structure for the models fitted in different scenarios are reflected on the oscillation frequencies, and we suggest which kind of observational data could give us enough information to constraint the evolutionary state of 12 Boo, and, possibly, also the properties of the transport processes (if any) in the stellar central region. Finally, in Sec. 5 we present our conclusions.

2 12 BOÖTIS: OBSERVATIONAL CONSTRAINTS

With the rapid development of optical interferometry in the last years, closer and closer binary systems have become resolvable. Thanks to interferometric orbits an increasing sample of double-lined spectroscopic binaries (SB2), including non-eclipsing systems, can be used for accurate stellar parameter determination. Interferometry essentially yields the orbital inclination that, combined with accurate radial velocity measurements, can provide mass determination at a level better than 1%, i.e. suitable for strict stellar modelling tests (see e.g. Andersen 1991).

A good example of an ideal target for this technique is 12 Boo, a bright ($V=4.83$) non-eclipsing SB2 with an orbital period of about ten days ($P = 9.6$) and a (composite) spectral type F8 IV -F9 IVw Barry (1970) (where “w” stays for weak metallic lines). Boden et al. (2005) obtained long baseline interferometry of 12 Boo with the Palomar Testbed Interferometer (PTI) and the Navy Prototype Optical Interferometer (NPOI). They secured, as well, new high resolution (echelle) spectra, as the previous spectroscopic observations (Abt & Levy 1976; De Medeiros & Udry 1999), were the major limit to the precision of derived parameters. The interferometric visibility data and the radial velocity curves were simultaneously solved to derive the orbital parameters. The components could not be resolved (the apparent orbital semiaxis is only 3.45 mas), so that the individual radii had to be derived by indirect means, namely by the Infrared Flux Method by Blackwell and collaborators (Blackwell et al. 1990; Blackwell & Lynas-Gray 1994). The information about the total and the individual bolometric fluxes (needed for radius determination) was derived by a fit of multi-wavelength archival data and from the in-band intensity ratio of the interferometric measurements. Furthermore, the analysis of the observed spectra provided an estimation of the component effective temperatures and of the luminosity ratio. A further improvement in the determination of the spectroscopic orbit by Tomkin & Fekel (2006), combined with the same interferometric data, confirms the values of the masses derived by Boden et al. (2005) and reduces the associated error bars. The relevant values

Table 1. Orbital parameters and magnitude differences for 12 Boo

Parameter	value	reference ^a
P (d)	$9.6045529 \pm 4.8 \cdot 10^{-6}$	1
e	0.19268 ± 0.00042	1
i	$107^\circ.99 \pm 0.077$	2
a (mas)	3.451 ± 0.018	2
ΔK_{CIT} (mag)	0.589 ± 0.005	2
ΔH_{CIT} (mag)	0.560 ± 0.020	2
ΔV (mag)	0.560 ± 0.020	2
K_A (Km s ⁻¹)	67.286 ± 0.037	1
K_B (Km s ⁻¹)	69.30 ± 0.050	1

^a References: 1) Tomkin & Fekel (2006), 2) Boden et al. (2005)

and their uncertainties are reported, for the reader's sake, in Table 1.

Other relevant information on the system are its near-solar chemical composition, with a mean value of $[\text{Fe}/\text{H}] = 0.01 \pm 0.08$, derived from Strömgren photometry and detailed spectroscopic analysis (Duncan 1981; Balachandran 1990; Lèbre et al. 1999; Nordström et al. 2004) and the component rotational velocities of 14.0 and 12.0 km s⁻¹ (Boden et al. 2005). The latter are slightly faster than the expected corotation rate of, respectively, 12.4 and 9.3 km s⁻¹.

The resulting global picture of 12 Boo is that of a binary with very similar components (masses, effective temperatures, rotation) except an unexpected magnitude difference: both spectroscopic and interferometric measurements indicate a difference of ~ 0.48 - 0.58 mag, depending on the band. That is quite hard to explain in a system with co-eval and non-interacting components (both of them are well inside the critical Roche lobe).

The high precision of the radial velocity measurements (the typical error is 0.5 km s⁻¹ in Boden et al. 2005; Tomkin & Fekel 2006) and the short orbital period rules out the possibility of making the masses unequal by "hiding" a small fraction of a component mass in a third unseen object. Unless rather improbable configuration of the third object orbit are assumed (i.e. orbit almost normal to the line of sight), even an object of a few hundredth solar masses orbiting one component would easily be detected from the reflex motion of the more massive companion. Besides, such a planetary orbit can be excluded on the ground of stability consideration, see e.g. Holman & Wiegert (1999) and references therein.

The observational constraints we assume in our modelling are taken from Table 5 of Boden et al. (2005) that, for the sake of convenience, we repeat here in Table 2. As the above mentioned spectroscopic and photometric studies of 12 Boötis indicate a metallicity within 0.1 dex of the solar value, given this uncertainty and a further uncertainty on the value of the solar metallicity, we adopted the solar Z/X of Grevesse & Noels (1993) considering a conservative error bar, as reported in Table 2.

Table 2. Observational constraints as adopted in the modelling.

	A	B
M/M_\odot	1.4160 ± 0.0049	1.3740 ± 0.0045
T_{eff} (K)	6130 ± 100	6230 ± 150
L/L_\odot	7.76 ± 0.35	4.69 ± 0.74
Z/X	0.0245 ± 0.01	0.0245 ± 0.01

3 MODELLING 12 BOÖTIS

In the following we will use the term "calibration" to denote the process of determining the stellar model parameters, such as initial composition and age (both the same for A and B components), satisfying - within 1- σ - the observational constraints: M_A , M_B , Z/X , L_A , L_B , $T_{\text{eff},A}$ and $T_{\text{eff},B}$.

As both system components are massive enough to develop a convective core during the main-sequence and no a-priori assumption on their evolutionary state can be made, the dependence of T_{eff} and luminosity on the stellar parameters (e.g. age and overshooting) is highly non-linear. As Boden et al. (2005) already pointed out, the result of system fitting strongly depends on the model details, and, in particular, on the amount of convective overshooting in the core.

The aim of this paper is to study the possible solutions (not just to find a single solution) and to verify the ability of discriminating among different scenarios. We apply, therefore, the minimization technique adopted and described in Miglio & Montalbán (2005) with the purpose of determining the chemical composition and age for each value of the overshooting parameter (assumed to vary from 0.0 to 0.50 in steps of 0.01). The parameters left free are: the initial chemical composition (described by the hydrogen and heavy-elements mass fraction, X and Z respectively), the age and the component masses. These are adjusted in order to fulfill the observational constraints in Table 2. A standard χ^2 is used as goodness-of-fit estimate, so that each observable is taken into account with its uncertainty. We did not allow α_{MLT} to be adjusted and fixed its value to $\alpha_{\text{MLT}} = 1.84$, i.e. the value provided by the Solar calibration. This choice is justified by the fact that both stars are quite close in the HRD and that different values of α_{MLT} are not expected. Besides, a variation of α_{MLT} implies a change of T_{eff} that can be easily balanced by a change of the chemical composition.

The search for a solution fulfilling the observational constraints on the HR diagram is usually biased by an additional criterion, though this is not included in the χ^2 : a preference towards long lasting evolutionary phases, as the probability of finding a star in a given evolutionary phase depends on how "rapid" that phase is. Evidently, it is less likely to observe a star in its second gravitational contraction than on the main sequence. This is however a statistical argument, that can be verified on large samples of stars (e.g. in clusters), but cannot be applied to a single case. In addition to that, the duration of each evolutionary stage depends on whether overshooting is considered in the models or not. As pointed out e.g. by Maeder (1975) and Noels et al. (2004), the duration of the thick-shell-hydrogen burning phase depends on the amount of overshooting as the latter increases the mass of the isothermal helium core

built during the core hydrogen-burning phase. As an example, a $1.4M_{\odot}$ star without overshooting spends in that phase $\sim 20\%$ of the main-sequence lifetime (see Iben 1991, for instance). An overshooting parameter $\alpha_{OV} \simeq 0.1$ implies a decrease of the duration of this evolutionary phase down to 4% of the main-sequence lifetime, i.e. lasting as long as the overall contraction phase. In our modelling we do not make, therefore, any a-priori assumption on the particular evolutionary phase of the solution.

Stellar Models

The stellar model sequences are computed with the code CLES (Code Liégeois d'Evolution Stellaire). The opacity tables are those of OPAL96 (Iglesias & Rogers 1996) complemented at $T < 10000$ K with Alexander & Ferguson (1994) opacities. The metal mixture used in the opacity tables, is the solar one according to Grevesse & Noels (1993). The nuclear energy generation routines are based on the cross sections by Caughlan & Fowler (1988) and updated with the recent measurement of the $^{14}N(p, \gamma)^{15}O$ reaction rate (Formicola et al. 2004). The weak screening factors come from Salpeter (1954), and the equation of state used in the computations is OPAL01 (Rogers & Nayfonov 2002). Convection transport is treated with the classical mixing length theory by Böhm-Vitense (1958) in the formulation by Cox & Giuli (1968); and atmospheric boundary conditions given by Kurucz (1998) are applied at $T = T_{\text{eff}}$.

Chemical mixing in the formal convective region and in the overshooting layer is treated as instantaneous. Besides, the thickness of the overshooting layer, Λ_{OV} , is expressed in terms of a parameter α_{OV} , so that $\Lambda_{OV} = \alpha_{OV} \times \min(r_{cv}, H_p(r_{cc}))$, where r_{cc} is the radius of the convective core. The temperature stratification in this overshooting layer could be radiative or adiabatic (e.g. Zahn 1991). At any rate the effect of this thin layer on the evolutionary track is very small, in our models a radiative stratification has been assumed.

We have computed as well models that, in contrast with the assumed instantaneous chemical mixing, include a diffusive treatment of mixing in the formal convective region and in the extra-mixed layer. These computations were done with the ATON3.0 code (D'Antona et al. 2005) for the same physics: MLT, OPAL1996 and Alexander & Ferguson opacities, as well as OPAL equation of state.

We have also studied (see Sect. 3.2) the effect of other chemical mixing processes, such as diffusion and gravitational settling of helium and heavy elements. Microscopic diffusion has been implemented in CLES code following the formulation by Thoul et al. (1994).

Finally, the effect of an additional turbulent mixing, such as the one expected to be induced by rotation, is addressed in Sec. 3.3.

3.1 Overshooting

We performed several calibrations for different values of the overshooting parameter and we found solutions with $\alpha_{OV} \geq 0.06$ (see. Table 3). By changing α_{OV} the evolutionary state of the system changes. In detail: for the lowest values of overshooting the situation is that represented in

Table 3. Parameters of the models.

	α_{OV}	Y_0	Z_0	Age (Gyr)
a	0.06	0.268	0.0195	3.08
b	0.15	0.267	0.0198	3.31
c	0.23	0.267	0.0200	3.58
d	0.37, 0.15	0.281	0.0186	3.24

Fig. 1.a: the primary component is close to the maximum luminosity in the shell-hydrogen burning phase, whereas the secondary, with a $X_c=0.03$, is at the end of its central hydrogen-burning phase. As α_{OV} increases, the evolutionary state of component A approaches the TAMS. With $\alpha_{OV} \simeq 0.15$ (Fig. 1.b) the primary is burning hydrogen in a thick shell while component B is well on the main sequence. A further increase of the overshooting parameter $\alpha_{OV} \geq 0.2$ places the primary in the rapid overall contraction phase (Fig. 1.c). Still larger values of α_{OV} make L_B increase out of $1-\sigma$ and therefore worsen the fit.

The observed luminosity ratio, $L_A/L_B \sim 1.65$ (from a minimum of 1.35 to a maximum of 2.) is the main obstacle for a solution with both components on the Main-Sequence. In fact, given that both components have the same age and initial chemical composition, if the same kind of mixing processes are considered in the center, the luminosity ratio in the main-sequence is determined by the mass ratio ($q \sim 0.97$), and does not significantly depend on the choice of the other common model parameters (X, Z, α_{OV}).

Regardless of the set (X, Z, α_{OV}) chosen, all the models computed with $\alpha_{OV,A} = \alpha_{OV,B}$ provided $(L_A/L_B)_{\text{MS}} \simeq 1.15$. A higher value of the luminosity ratio can be reached if $\alpha_{OV,A} > \alpha_{OV,B}$. Therefore, the only way we found to place both components in their MS phase is to assume a different efficiency of mixing processes in each component. In Fig. 1.d we show a calibration solution obtained by assuming $\alpha_{OV,A} \simeq 0.37$ and $\alpha_{OV,B} \simeq 0.15$. In this case both 12 Boo A and B are well in the MS.

The values of stellar parameters collected in Table 3 are those used in the figures and comparisons in this paper. It has to be noticed, however, that the uncertainty on Z/X reflects on an uncertainty of 0.02 in the initial helium mass fraction (Y_0) and of 0.2 Gyr in the age of the models. Besides, the calibrations with $\alpha_{OV,A} = \alpha_{OV,B}$ and similar initial chemical composition provide an age difference of the order of 15%, and the calibration with $\alpha_{OV,A} > \alpha_{OV,B}$ implies an age in the range bracketed by the $\alpha_{OV,A} = \alpha_{OV,B}$ models. Unfortunately, the uncertainty in Z/X is too large to constrain the models.

All the different scenarios presented here cannot be clearly discriminated by means of the available observational constraints, nevertheless, the internal structure of these models are significantly different, and these differences shall show up in their asteroseismic properties (see. Sec. 4).

Diffusive overshooting

The classical treatment of overshooting is an extension of the instantaneously mixed convective core by a distance Λ_{OV} . In the diffusive approach of convection, chemical mixing is described by the diffusion equation with diffusion coefficient

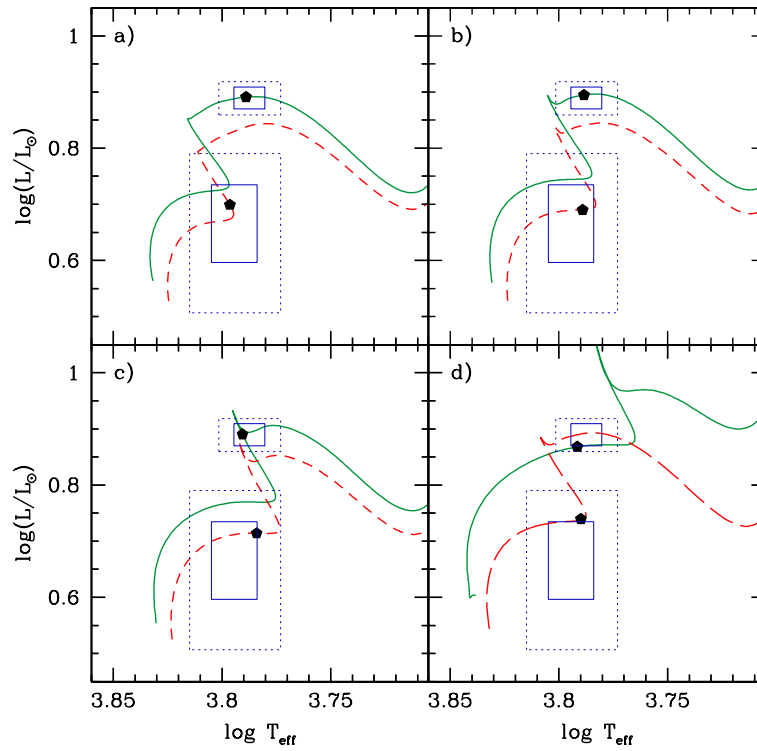


Figure 1. HR diagram showing solutions found with different values of the overshooting parameter: *a)* $\alpha_{OV} = 0.06$, *b)* $\alpha_{OV} = 0.15$, *c)* $\alpha_{OV} = 0.23$, and *d)* $\alpha_{OV,A} = 0.37$ and $\alpha_{OV,B} = 0.15$. Model parameters are described in Table 3. Error boxes corresponding to 1- and 2- σ error bars in L and T_{eff} are represented by continuous and dotted lines.

$D = 1/3 v_{\text{conv}} \Lambda$, where v_{conv} is the average turbulent velocity and Λ the convective scale length. In a MLT treatment $v_{\text{conv}} \propto (\nabla - \nabla_{\text{ad}})$ and $\Lambda \propto H_p$, which imply $v_{\text{conv}} = 0$ at the formal boundary of the convective region ($\nabla = \nabla_{\text{ad}}$). In order to define a continuous diffusion coefficient, also in the overshooting region, ATON code extrapolates the $\log v_{\text{conv}}$ vs. $\log P$ relation, to get the turbulent velocity at the boundary, starting from a point inside the convective region where the pressure is 5% larger than at the boundary. Furthermore, following Xiong (1985), turbulent velocity is assumed to exponentially vanish outside the convective region, and the thickness of the mixed region is determined by the parameter β which describes the exponential vanishing of turbulent velocity. As shown by Ventura et al. (1998), a β value ten times smaller than the α_{OV} in classical instantaneous mixing produces the same effect on the HR diagram.

With this formulation of overshooting we find the same set of solutions as with instantaneous mixing, this time for a parameter β in the range 0.004-0.035. This is of course reassuring as a completely independent stellar evolution code, and a different description of overshooting have been used. The chemical composition profiles at the border of the convective core are, however, much smoother with the diffusive overshooting than with the classical treatment.

3.2 Effects of diffusion

Richard et al. (2001), Michaud et al. (2004) and Richard

(2005) showed that microscopic diffusion can affect the size and evolution of a convective core. In those papers, thermal diffusion, gravitational settling and radiative accelerations were included in the models to derive the evolution of chemical distribution. CLES code does not take radiative accelerations into account. Nevertheless, there is no observational evidence in 12 Boo of surface chemical peculiarities that could be produced by gravitational-settling and radiative-acceleration, and the latter is not expected to play a mayor role in the central region (see e.g. Richard et al. 2001).

We do not expect a large effect of radiative acceleration in the 12 Boo mass domain, since the thickness of their convective envelopes is quite large. Even if at the beginning of the MS component A has a shallow convective envelope, and therefore the role of radiative accelerations could be non-negligible, as the star evolves its convective region becomes deeper. As a consequence, the effect of radiative acceleration is reduced, and the chemical composition of the convective region re-homogenized. We decided, therefore, to consider and compare models accounting for diffusion of H and He, and of H, He and Z.

Michaud et al. (2004) showed that microscopic diffusion can induce an increase of the convective core for a narrow range of masses, from 1.1 to 1.5 M_{\odot} , and that the effect decreases rapidly with increasing stellar mass. We also note that in this mass domain, the convective core mass increases during the MS evolution instead of decreasing, as it occurs for larger masses. As a consequence, a sharp gradient of

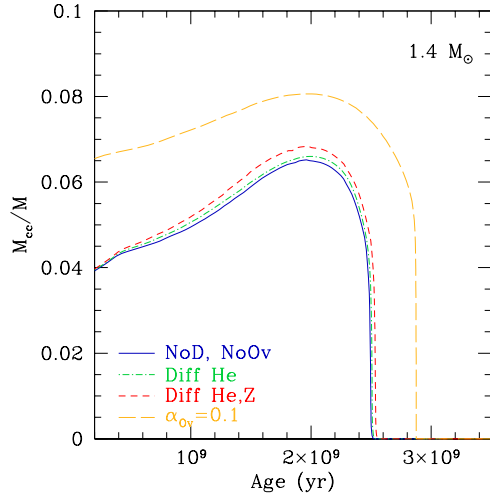


Figure 2. Fractional mass of the convective core as a function of the age in no diffusion models: without overshooting (solid line) and with $\alpha_{ov} = 0.1$ (long-dashed line); and in no overshooting models including microscopic diffusion of He and H (dashed-dotted line) and of He, H and Z (dashed line).

chemical composition appears at the convective core border, making the diffusion process much more efficient in that region.

As shown in Fig. 2, for a $1.4 M_{\odot}$ star, the increase of the core mass fraction when diffusion of H, He and Z is considered is of only $\simeq 5\%$, and the age of the turnoff is only slightly increased (Fig. 3). This is in agreement with the findings of Michaud et al. (2004) and Richard (2005) who consistently included radiative accelerations in their computations while considering Z-diffusion. An obvious consequence is that, in presence of diffusion, the amount of overshooting needed to find 12 Boo A and B in a given evolutionary state is reduced with respect to the values obtained in the previous section. In fact, the minimum amount of overshooting required is slightly smaller, i.e. $\alpha_{ov} \simeq 0.04$ instead of 0.06. The evolutionary state of the calibrated system changes, with increasing α_{ov} , in a way similar to that described Sec. 3.1.

On the other hand, the increase of the opacity in the envelope due to the settling of He and Z provides evolutionary tracks cooler than those without diffusion (this effect is even more important if only H and He diffusion is considered, see Fig. 3). At the end of the main sequence the surface Z/X is $\sim 10\%$ (diffusion of H and He) or $\sim 25\%$ (diffusion of H, He and Z) smaller than the initial value, nevertheless, given the uncertainties in the observed Z/X , this implies only a slight change in the Z and X initial values in the calibrated models.

In addition to a slight enlargement of the convective core, diffusion leads to a smoother chemical composition profile at the edge of the convective core (see Fig. 10). Whether this property affects the oscillation modes of the components will be addressed in see Sec. 4.

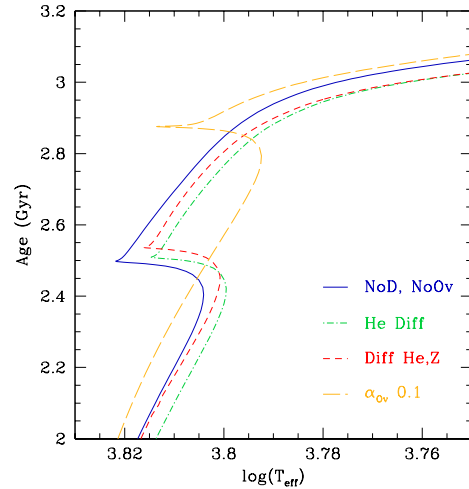


Figure 3. Evolutionary tracks of the models described in Fig. 2 in a $\log T_{\text{eff}}$ -Age diagram.

3.3 Other sources of extra-mixing in the core

The shear instability induced by stellar rotation is considered as one of the first causes of chemical mixing in the radiative interior of the stars. Different approaches have been proposed to treat the effects of rotation on transport of angular momentum and chemicals (see Maeder & Meynet 2000; Mathis et al. 2004, for a review). Since our stellar evolution code does not include a consistent treatment of rotational effects, we simply include the chemical turbulent mixing by adding a turbulent diffusion coefficient (D_T) in the diffusion equation. In our parametric approach D_T is assumed to be constant inside the star and independent of age. These simple prescriptions are inspired by the results obtained by Mathis et al. (2004) from a consistent study of rotational effects in a $1.5 M_{\odot}$ star (see their Fig. 2).

We have then calibrated our models with different values of D_T . We find, similarly to the case of including overshooting (see Sec. 3.1), that we are able to fit the system at different evolutionary stages depending on the value of D_T ; the values needed to fit the system are in the range $30 - 170 \text{ cm}^2 \text{ s}^{-1}$. We note that these values are of the same order of the total diffusion coefficient resulting from the calculations for a $1.5 M_{\odot}$ model as presented in Mathis et al. (2004). As already seen for overshooting, in order to fit the system with 12 Boo A and B in their main-sequence, a different efficiency of mixing must be assumed in each component: $D_{T,A} = 330 \text{ cm}^2 \text{ s}^{-1}$, and $D_{T,B} = 120 \text{ cm}^2 \text{ s}^{-1}$.

The simplified parametric treatment of rotationally induced mixing used in this work has the aim of showing that if an extra-mixing process, different from overshooting, is acting near the core it will produce a different chemical composition profile in the central regions of the star. Whether these different profiles are reflected or not on the solar-like oscillations features will be analysed in Sec.4.2.

4 ASTEROSEISMIC PROPERTIES

Stellar models predict the presence of a convective envelope for the range of masses of 12 Boo A and B and, therefore, solar-like oscillations are expected to be excited in both components of the system. By means of the scaling relations of Kjeldsen & Bedding (1995), Kjeldsen & Bedding (2001) and the theoretical predictions of Houdek et al. (1999), and using the precisely determined values of the mass and the luminosity, we estimate that the modes with the largest amplitudes should be around $\nu_{\max} = 700 \mu\text{Hz}$ and $\nu_{\max} = 1200 \mu\text{Hz}$ in 12 Boo A and B, respectively. The peak amplitude in the power-spectrum is expected to be 3-4.5 times larger than the solar-one for the A component, and 2.5-3.5 times larger than the solar one for the B component.

The components of 12 Boötis are massive enough to develop a convective core during main sequence. The combined action of nuclear burning and convective mixing is responsible for the development of a steep chemical composition gradient at the boundary of the convective core. As a star leaves the main-sequence, the increasing central condensation, together with the steep chemical composition gradient in the central regions, leads to a large increase of the buoyancy frequency (N) and, therefore, of the frequencies of gravity modes. The latter interact with pressure modes and affect the properties of non-radial solar-like oscillations by the so-called *avoided crossing* phenomenon (see e.g. Osaki 1975; Aizenman et al. 1977). The frequency of the modes undergoing an *avoided crossing* (also called mixed-modes) are therefore sensitive probes of the core structure of the star.

As a first example let us consider the evolution of the frequencies of the model of component A corresponding the scenario *b* of Table 3 (hereafter *Ab*). In Fig. 4 we plot the evolution of frequencies for $\ell = 0$ (dotted lines) and $\ell = 1$ (solid lines) modes, and show how *g*-modes, whose frequency strongly increases after the overall contraction (~ 3.27 Gyr), interact with pressure modes of same degree. This interaction results in non-radial modes with a mixed *p*- and *g*-character and frequencies that significantly deviate from a regular spacing between consecutive overtones.

Since the thickness of the mode evanescent region (where $N < \omega < S_\ell$, with S_ℓ being the so-called Lamb frequency) increases with the degree ℓ (see propagation diagram in Fig. 5), the interaction between *p* and *g* modes decreases. As a consequence, in modes of degree $\ell > 1$, the behaviour of gravity and pressure mode is generally better separated (see e.g. Christensen-Dalsgaard et al. 1995; Morel et al. 2001): *g*-modes tend to remain concentrated in the core and would hardly be detectable due to their significantly larger inertia. This is in fact the case for the our models *Aa* and *Ab* where only $\ell = 1$ modes present a mixed character. Nevertheless, for the less evolved models (*Ac* for instance) also $\ell = 2$ mixed modes appear in the solar-like frequency domain. In the following discussion we will address mainly the properties of mixed modes.

Given the MS status of 12 Boo B, we will first discuss the seismic properties of component A, and only in Sec. 4.1.1 consider the additional information that the observation of solar-like oscillations of component B would add to the modelling.

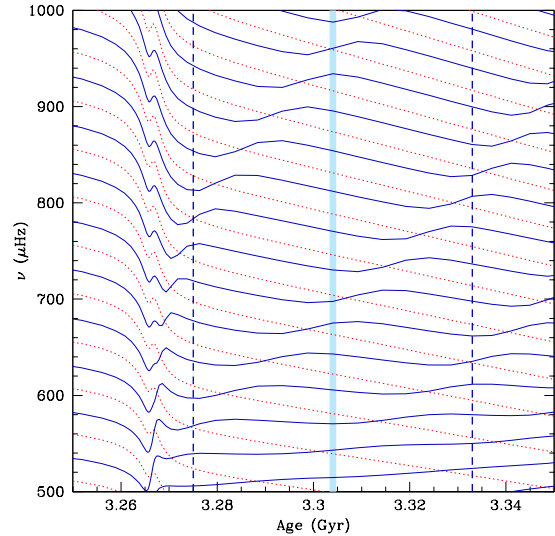


Figure 4. Evolution in time of the frequencies of model *Ab*. Dotted and solid lines represent radial and $\ell = 1$ modes with radial order n from 11 to 23. The frequencies of model *Ab* are highlighted by a thick vertical line. Vertical dashed lines represent $\pm 1 \sigma$ interval in the observed T_{eff} .

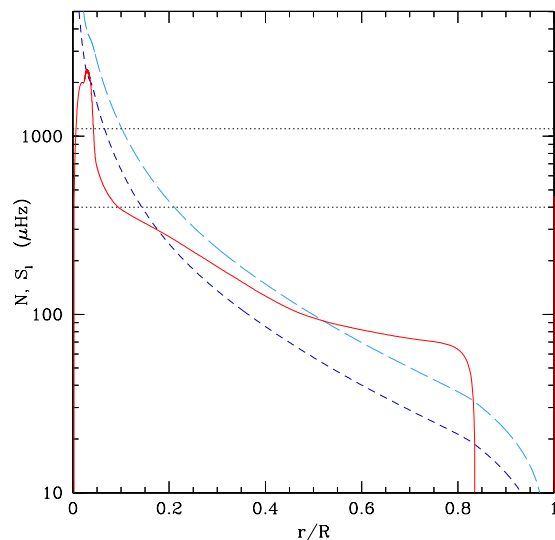


Figure 5. Propagation diagram for model *Ab* (see Table 3, Fig. 1). The solid line represents the Brunt-Väisälä frequency N , the short- and long-dashed line the Lamb frequency S_ℓ for, respectively $\ell = 1$ and $\ell = 2$. The domain of solar-like oscillations falls within the horizontal dotted lines.

4.1 Probing the evolutionary status

As already investigated in the case of η Boötis (see e.g. Di Mauro et al. 2004), the frequencies of modes undergoing an *avoided-crossing* are direct probes of the evolutionary status of intermediate mass stars.

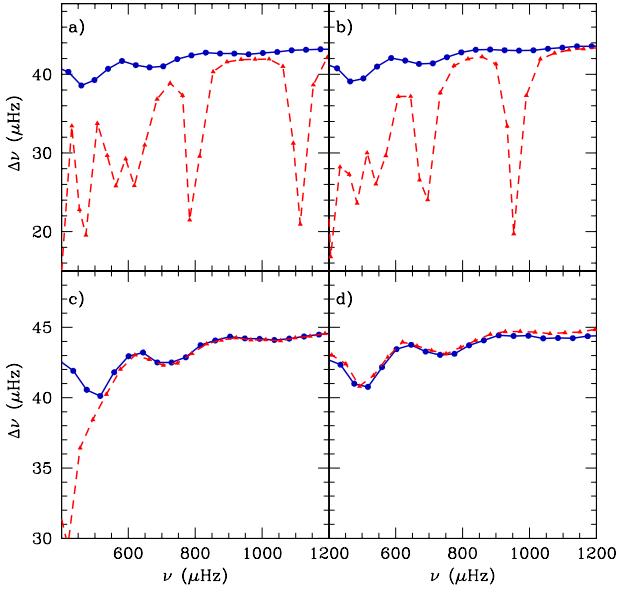


Figure 6. Large frequency separation as a function of the frequency for the models described in Fig. 1. Solid and dashed lines connect, respectively, $\Delta\nu$ for radial and $\ell = 1$ modes.

In Fig. 6 we compare the large frequency separation¹ $\Delta\nu$ for radial and $\ell = 1$ modes corresponding to the models of component A presented in Fig. 1. Though radial modes do not give information on the evolutionary status, $\ell = 1$ modes allow a clear discrimination among the scenarios. Modes of mixed p and g character are not present in the model on the main sequence (Fig. 6.d) and $\Delta\nu$ is almost constant, indicating therefore a regular spacing between modes of consecutive radial order (both radial and $\ell = 1$). On the other hand, as more evolved models (Aa, Ab and Ac) are considered, the *avoided crossings* effects become more evident. Therefore, for the model in the second overall contraction (Ac, Fig. 6.c) the interaction between p and g modes changes by up to $10 \mu\text{Hz}$ the modes with frequencies lower than $600 \mu\text{Hz}$ (corresponding order-mode, n , lower than 12). That can also be seen in Fig. 4 for models at 3.265 Gyr and the lowest n modes. For more evolved models (Aa and Ab) the avoided crossing phenomenon clearly breaks the regular frequency spacing in the domain of expected solar-like oscillation (Figs. 6.a and 6.b).

The radical variation of the properties of $\ell = 1$ modes derives from a considerable change of the Brunt-Väisälä frequency near the center of the star (see Fig. 7) as hydrogen is exhausted throughout the convective core and the star undergoes an overall contraction. As models of component A at different evolutionary stages are obtained for different amounts of core overshooting, the detection of mixed modes and their frequencies would allow to constraint the value of the overshooting parameter or the extension of the mixed central region. While model Aa (computed with $\alpha_{\text{OV}} = 0.06$) presents *avoided crossings* at $\nu = 780 \mu\text{Hz}$ ($n = 15$) and $\nu = 1100 \mu\text{Hz}$ ($n = 24$) model Ab ($\alpha_{\text{OV}} = 0.15$)

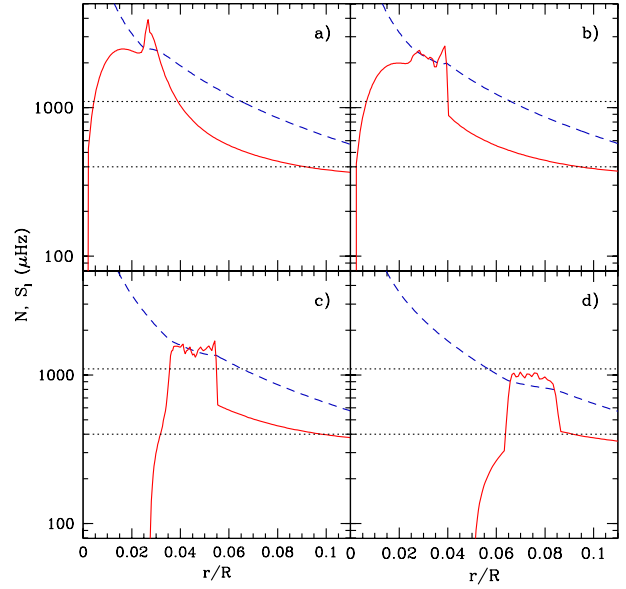


Figure 7. Propagation diagram in the core of the models for which large frequency separation has been plotted in Fig. 6. Solid line represents the Brunt-Väisälä frequency, and the dashed line the Lamb frequency for $\ell = 1$.

does it at $\nu = 700 \mu\text{Hz}$ ($n=13$) and $\nu = 950 \mu\text{Hz}$ ($n=20$). These differences between the frequencies of the modes presenting mixed p-g character ($\sim 100 \mu\text{Hz}$), as well as the differences of the frequency spacing between two consecutive avoided crossings ($\sim 20 \mu\text{Hz}$), are large enough to be detected with the current observational techniques. Furthermore, 12 Boo A has a rotational velocity 14 km s^{-1} (Boden et al. 2005) that, assuming an inclination of the rotational axis equal to the orbital one (108°), implies a rotational splitting between ($\ell = 1, m = -1$) and ($\ell = 1, m = 1$) modes of only $2.5 \mu\text{Hz}$.

Distinguishing between scenarios Ac ($\alpha_{\text{OV}} = 0.23$) and Ad ($\alpha_{\text{OV}} = 0.37$ for 12 Boo A and $\alpha_{\text{OV}} = 0.15$ for 12 Boo B) on the base of $\ell = 1$ mixed modes might be less straightforward since the effect of avoided crossing occurs at lowest frequencies, where the amplitudes of the modes are predicted to be small. Therefore, no detection of avoided crossing could imply, either that 12 Boo A is well in MS, and has therefore a large central mixed region, or that it is close to the TAMS. Luckily, for models in the second overall contraction (SOC), the changes in stellar structure are such that $\ell = 2$ mixed modes appear in the predicted solar-like spectrum, while for MS models (Ad) they would have very low frequencies.

4.1.1 Seismology of component B

Though in all calibrations we considered component B as a main-sequence object and, therefore, avoided crossings are not expected, the detection of solar-like oscillations in the secondary would, nonetheless, add constraints to the modelling of the binary system. A first additional constraint comes from the average value of the large frequency separation ($\langle\Delta\nu\rangle$) that, for main-sequence stars, is well known to

¹ Computed as the difference between modes of same degree and consecutive frequencies.

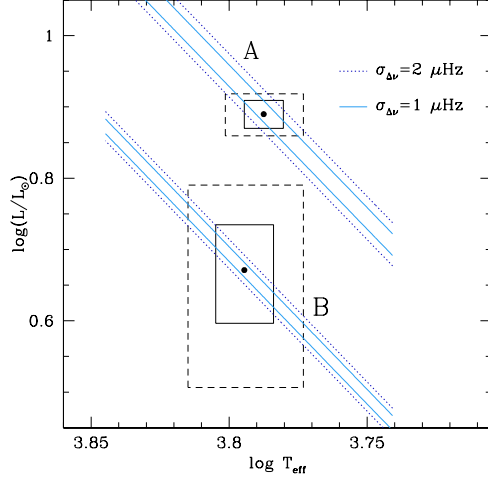


Figure 8. Position in the HR diagram of 12 Boo A and B with 1 and 2- σ error boxes in $\log L$ and $\log T_{\text{eff}}$. Also shown are lines of constant radius deduced from the (known) masses of the components and the large frequency separation. The large separation is assumed to be known with an uncertainty of 1 (continuous lines) and 2 μHz (dotted lines).

represent an estimate of the mean density and, hence, of the stellar radius, if the mass is known. The available estimate of component radii in 12 Boo (Boden et al. 2005) is based on the Infrared Flux method and yields: $R_A = 2.474 \pm 0.096 R_\odot$ and $R_B = 1.86 \pm 0.15 R_\odot$. However, a more precise and independent determination of the stellar radii could be obtained, thanks to the small uncertainty on the masses (0.3%), from the knowledge of $\langle \Delta\nu \rangle$. In particular for component B, the measurement of $\langle \Delta\nu \rangle$, would result in a significantly smaller uncertainty on its location in the HR diagram and, therefore, in tighter constraints on the modelling. In Fig. 8 we show the uncertainty on the radii deriving from $\langle \Delta\nu \rangle$ values supposed to be known with an accuracy of 1 and 2 μHz .

Information on the central structure of component B could be provided by the small frequency separations $\delta\nu_{02}$. In Fig. 9 we show $\delta\nu_{02}$ as a function of the frequency, as expected for the models of 12 Boo B corresponding to the four scenarios of Fig. 1. We notice that the dependence of $\delta\nu_{02}$ on ν is mainly determined by the location of the discontinuity in sound speed derivative at the border of convective core, while the age of the model changes the mean value of $\delta\nu_{02}$. The spread of $\delta\nu_{02}$ for the four considered scenarios increases with the frequency and is of the order of 2 μHz at 1500 μHz and of 1.5 μHz at ν_{max} . The age difference between scenarios *b* and *d* (note that both have $\alpha_{\text{OV}} = 0.15$) implies a shift of only 0.5 μHz in $\delta\nu_{02}$.

Can $\delta\nu_{02}$ of component B help to discriminate between scenarios *c* and *d* in absence of avoided crossing detection? Fig. 9 shows that the difference of $\delta\nu_{02}$ at ν_{max} is only 0.2 μHz and reaches 0.5 μHz at 1500 μHz . Furthermore, the frequency of $\ell = 2$ modes will be affected by rotational splitting (expected to be $\sim 1 - 1.5 \mu\text{Hz}$), so that an accurate and reliable measurement of the small separation (expected to be around 3 μHz) will be a rather difficult task. Other frequency combinations, such as the small separation d_{01} are known to be very sensitive to the core structure of main se-

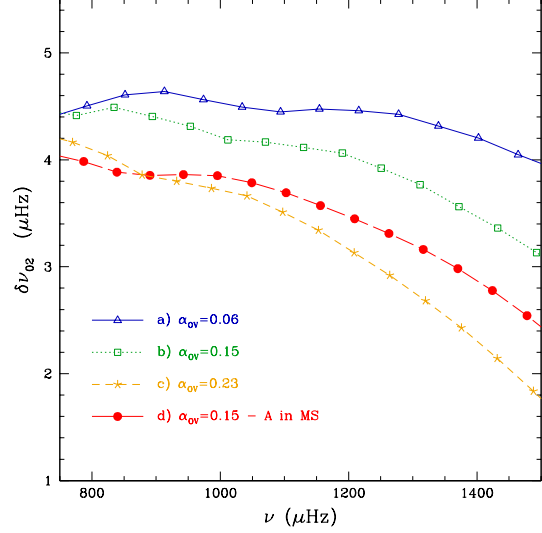


Figure 9. The small frequency separation $\delta\nu_{02}$ as a function of frequency in models of component B corresponding to the scenarios *a* – *d* described in Fig. 1.

quence stars (see e.g. Roxburgh & Vorontsov 2003 and references therein), but the larger number of frequencies needed to compute these small differences, increases even more their observational uncertainty.

4.2 Probing the chemical composition gradient in the core

Is there any other information that the knowledge of the frequency of an avoided crossing can give us? The appearance of avoided crossings is due to the evolution of frequencies of gravity modes and their interaction with acoustic modes of similar frequency. The frequency spectrum of gravity modes, on its turn, is mainly determined by the behaviour of N in the central regions of a star ($\nu \propto \int N/r dr$). Furthermore, the mean molecular weight gradient (∇_μ) is determined by the evolutionary state, but it can be also modified by different mixing processes taking place in the radiative interior. If the N profile changes because of a different ∇_μ , then we could expect a signature in the *avoided crossings* frequencies.

In each of the evolutionary states *a* – *d* we considered, the different mixing processes we analyse (classical and diffusive overshooting, microscopic and turbulent diffusion) provide models with a central structure showing a different ∇_μ and therefore different N profiles. In Fig. 10 we plot the hydrogen mass fraction and N profiles in the central region of 12 Boo A models in the evolutionary states *b* and *c* resulting from the calibrations with classical overshooting, with (short-dashed lines) and without microscopic diffusion (solid lines), and calibration with turbulent diffusion (long-dashed lines). Though the evolutionary state is the same, the difference of chemical composition gradient (Fig. 10 upper panels) is clearly reflected on the Brunt-Väisälä frequency profile (Fig. 10 lower panels), and therefore on the frequency of g-modes and on the properties of the avoided crossings (see Fig. 11). Consequently, the determination of mixed-

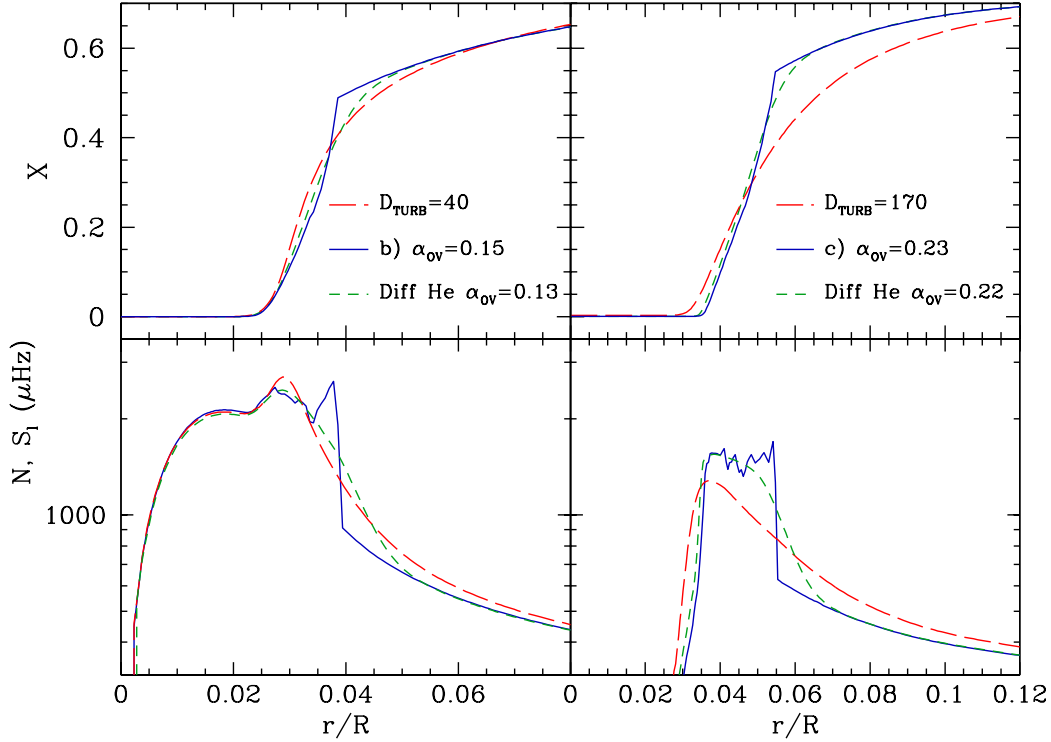


Figure 10. Hydrogen profile (*upper panel*) and Brunt-Väisälä frequency (*lower panel*) in models computed with overshooting (continuous line), with turbulent mixing (long-dashed line) and with diffusion of H and He (short-dashed lines)

mode frequencies with a precision better than $\sim 2 \mu\text{Hz}$ for frequencies around $650 \mu\text{Hz}$, would allow to determine the properties of the chemical composition profile and, hence, of the physical mechanism responsible for the extra-mixing outside the core. The effect of different $\nabla\mu$ is even larger at lower frequencies: at $500 \mu\text{Hz}$, where the expected mode amplitude is slightly larger than half of the amplitude at ν_{max} , the difference between overshooting and D_{T} models reaches $5 \mu\text{Hz}$.

We notice that such a valuable inference on the properties of the chemical composition gradient is made possible, in the example presented here above, by a trade-off between two effects. On one hand, the difference in $\nabla\mu$, which is due to a different mixing process, decreases as we consider more evolved models. On the other hand, the number of g modes entering the domain of solar-like oscillations, and therefore the number of avoided crossings, increases as the model evolves. This is the reason why, even though the differences between chemical composition profiles provided by classical overshooting and by D_{T} models increase as we consider less evolved models (see Fig. 10, lower panel), the lack of $\ell = 1$ avoided crossing predicted in the domain of solar-like oscillations for the scenarios *c* and *d*, makes difficult to infer information on the detailed properties of the μ gradient.

As mentioned above, models in the second gravitational contraction present $\ell = 2$ avoided crossings in the solar-like spectrum domain. These $\ell = 2$ modes are however less sensitive than $\ell = 1$ modes to the N profile, and the difference between overshooting and microscopic diffusion profiles is

not large enough to be reflected in $\ell = 2$ frequency modes. Models in the scenario *c* including turbulent diffusion show, however, very different N in the central region, in particular, the model reaches the same location in the HR diagram with a smaller convective core, and this is reflected on a difference in the frequency of modes undergoing an avoided crossing, of the order of $100 \mu\text{Hz}$ with respect to those in the overshooting models.

Concerning the main-sequence calibrated models (both for A and B components) we note that while in overshooting models $\delta\nu_{02}$ as a function of ν has a slope increasing with the value of the overshooting parameter, for turbulent diffusion models, $\delta\nu_{02}$ shows only a weak ν -dependence. That can be explained in terms of a different effect on the size of the convective core. While, in fact, in overshooting models the increase of α_{ov} implies a larger core, in turbulent diffusion ones the increase of D_{T} parameter decreases $\nabla\mu$ at the border of the convective core, but leaves the core radius almost unaffected. Besides, the convective core for 12 Boo stellar masses is too small, and the difference between $\delta\nu_{02}$ slope for overshooting and D_{T} models not large enough to be detected in the expected solar-like frequencies.

The effect of other diffusion processes such as the diffusive overshooting or the microscopic diffusion on the μ -profile and on the frequencies of the avoided crossings are similar to those described for the turbulent mixing. The effect of microscopic diffusion is, however, not limited to the core: it also modifies the structure of the envelope by a decrease of the helium abundance in the outer convective zone and by the appearance of a chemical composition gradient

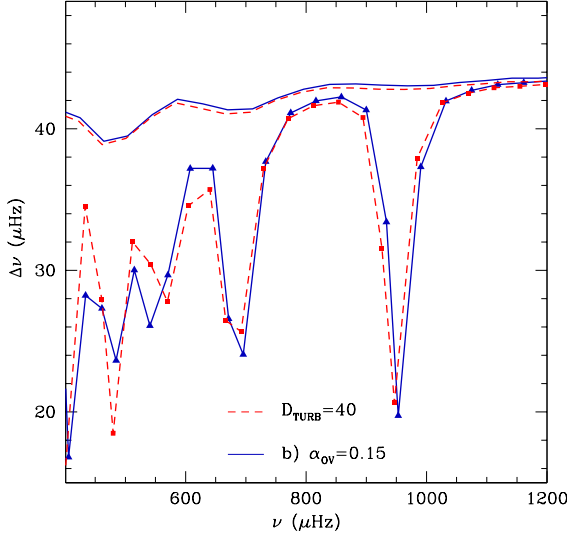


Figure 11. $\ell = 0$ and $\ell = 1$ large frequency separation in models of which chemical gradient and Brunt-Väisälä are plotted in Fig. 10. Model Ab with overshooting $\alpha_{OV} = 0.15$ (continuous line), and model with turbulent mixing (long-dashed line). The different chemical composition gradient (see Fig. 10) affects the frequencies of $\ell = 1$ modes undergoing avoided crossings (lower curves) but not the frequencies of radial modes (upper curves).

below the convective envelope. The combination of these effects leaves, as noticed e.g. in Théado et al. (2005), a clear signature in the frequencies of acoustic modes. In order to fully exploit this seismic signature a high frequency resolution, that only long and uninterrupted observations can provide, is however needed.

5 CONCLUSIONS

We have presented a detailed modelling of the binary system 12 Boötis by fitting the available observational constraints: effective temperatures, luminosities, chemical composition, and high precision masses of both components. As result of different 12 Boo calibrations we found a set of possible theoretical scenarios where the secondary is on the main sequence, whereas the primary has already left it. Its precise evolutionary state, however, may vary from the SOC (models Ac) to a thick-shell-H-burning phase (models Aa) by varying the overshooting parameter α_{OV} from 0.23 to 0.06. These values slightly decrease (by 0.02) if microscopic diffusion is included in stellar modelling. Other central mixing processes, such as diffusive overshooting (described by the β parameter), and a turbulent mixing with a parametric turbulent diffusion coefficient (D_T) lead to the similar results. For each transport processes we found a possible range of values of the parameters α_{OV} , β and D_T that place 12 Boo B in the MS and 12 Boo A between the second gravitational contraction and the sub-giant phase. The only way to place both components in the MS (models Ad) is to assume a different efficiency of the mixing process in both components, for instance : $\alpha_{OV,A} = 0.37$, $\alpha_{OV,B} = 0.15$, or $D_{T,A} = 330 \text{ cm}^2 \text{ s}^{-1}$, $D_{T,B} = 100 \text{ cm}^2 \text{ s}^{-1}$. With the avail-

able observational constraints we are not able, however, to discriminate among the different scenarios and models proposed: it is clear that additional and independent observational constraints are needed.

In Sec. 4 we have shown that the detection of the theoretically predicted solar-like oscillations in 12 Boötis would provide a powerful test to discriminate between different scenarios. Indeed, the detection of avoided crossings in the primary oscillation spectrum will allow a robust inference on the evolutionary state of the star and, therefore, on the amount of overshooting (or extra-mixing) from the core. The presence or absence of $\ell = 1$ mixed modes will allow to discriminate between sub-giant and MS models, and the absence of both $\ell = 1$ and $\ell = 2$ will allow to place 12 Boo A in the MS, before the SOC. This possibility is especially exciting since it would imply that, even for stars with masses so close, the central mixing has might have been working with a significantly different efficiency, opening the door to important questions concerning transport processes.

As shown in Sec. 4.2, for a model in a given evolutionary state, a different chemical composition profile in the core can be due to a different physical process responsible for the extra-mixing. This affects the behaviour of the Brunt-Väisälä frequency and hence the frequency of modes of mixed p- and g- character. Consequently, information on the mixing process taking place in the stellar center could be inferred from the mixed mode frequencies. The precision required to reach this goal is, however, evolutionary state dependent. While for a thin-shell-H-burning phase, a precision of $2 \mu\text{Hz}$ should be enough to distinguish between the sharp chemical profile provided by overshooting and the smoother one from a diffusive process, in a slightly more evolved phase (thick-shell-H-burning phase) the effect would be already erased. On the other hand, as stellar age decreases, the number of mixed modes also decrease. As consequence, for models in the second gravitational contraction, information on the mixing process can be derived from $\ell = 2$ mixed modes only if the generated chemical profiles are quite different. For MS models, where no avoided crossings are predicted, the effect of the central mixing on the small separation $\delta\nu_{02}$ is not large enough to distinguish between different transport processes.

Finally, the detection of solar-like oscillations also in the B component, will reduce the uncertainties on the HR location of 12 Boo B, and hence will significantly improve the observational constraints of the system. Nevertheless, as all the models of component B are in the MS, no useful information concerning the age of the system will be added by the 12 Boo B frequencies.

In conclusion, we have shown that thanks to the precise knowledge of the masses of 12 Boötis, and the additional constraints due to the binarity, the search and detection of solar-like oscillations in 12 Boo, hopefully by a spectroscopic multi-site campaign of observations, would mean an important step in the understanding of stellar evolution in the mass domain where the convective core appears.

ACKNOWLEDGEMENTS

A.M and J.M acknowledge financial support from the Prodex-ESA Contract Prodex 8 COROT (C90199). CM thanks funding from COFIN 2004-Asteroseismology.

REFERENCES

- Abt H. A., Levy S. G., 1976, *ApJS*, 30, 273
- Aizenman M., Smeyers P., Weigert A., 1977, *A&A*, 58, 41
- Alexander D. R., Ferguson J. W., 1994, *ApJ*, 437, 879
- Andersen J., 1991, *A&A Rev.*, 3, 91
- Andersen J., Clausen J. V., Nordstrom B., 1990, *ApJ*, 363, L33
- Böhm-Vitense E., 1958, *Zeitschrift für Astrophysics*, 46, 108
- Balachandran S., 1990, *ApJ*, 354, 310
- Barry D. C., 1970, *ApJS*, 19, 281
- Bedding T. R., Kjeldsen H., Butler R. P., McCarthy C., Marcy G. W., O'Toole S. J., Tinney C. G., Wright J. T., 2004, *ApJ*, 614, 380
- Blackwell D. E., Lynas-Gray A. E., 1994, *A&A*, 282, 899
- Blackwell D. E., Petford A. D., Arribas S., Haddock D. J., Selby M. J., 1990, *A&A*, 232, 396
- Boden A. F., Torres G., Hummel C. A., 2005, *ApJ*, 627, 464
- Bouchy F., Bazot M., Santos N. C., Vauclair S., Sosnowska D., 2005, *A&A*, 440, 609
- Bouchy F., Carrier F., 2002, *A&A*, 390, 205
- Carrier F., Bourban G., 2003, *A&A*, 406, L23
- Caughlan G. R., Fowler W. A., 1988, *Atomic Data and Nuclear Data Tables*, 40, 283
- Chiosi C., 1998, in Aparicio A., Herrero A., Sánchez F., eds, *Stellar astrophysics for the local group: VIII Canary Islands Winter School of Astrophysics Fundamentals of Stellar Evolution Theory: Understanding the HRD*. p. 1
- Christensen-Dalsgaard J., Bedding T. R., Kjeldsen H., 1995, *ApJ*, 443, L29
- Cox J. P., Giuli R. T., 1968, *Principles of Stellar Structure*. Gordon and Breach
- D'Antona F., Cardini D., Di Mauro M. P., Maceroni C., Mazzitelli I., Montalbán J., 2005, *MNRAS*, 363, 847
- De Medeiros J. R., Udry S., 1999, *A&A*, 346, 532
- Di Mauro M. P., Christensen-Dalsgaard J., Paternò L., D'Antona F., 2004, *Sol. Phys.*, 220, 185
- Duncan D. K., 1981, *ApJ*, 248, 651
- Formicola A., Imbriani G., Costantini H., Angulo C., Bemmerer D., Bonetti R., Brogini C., Corvisiero P., Cruz J., Descouvemont P., Fülöp Z., Gervino G., Guglielmetti A., Gustavino C., et al. 2004, *Physics Letters B*, 591, 61
- Grevesse N., Noels A., 1993, in Hauck B. Paltani S. R. D., ed., *La formation des éléments chimiques, AVCP La composition chimique du soleil*. pp 205–257
- Holman M. J., Wiegert P. A., 1999, *AJ*, 117, 621
- Houdek G., Balmforth N. J., Christensen-Dalsgaard J., Gough D. O., 1999, *A&A*, 351, 582
- Iben I. J., 1991, *ApJS*, 76, 55
- Iglesias C. A., Rogers F. J., 1996, *ApJ*, 464, 943
- Kjeldsen H., Bedding T. R., 1995, *A&A*, 293, 87
- Kjeldsen H., Bedding T. R., 2001, in Wilson A., Pallé P. L., eds, *ESA SP-464: SOHO 10/GONG 2000 Workshop: Helio- and Asteroseismology at the Dawn of the Millennium Current status of asteroseismology*. pp 361–366
- Kjeldsen H., Bedding T. R., Butler R. P., Christensen-Dalsgaard J., Kiss L. L., McCarthy C., Marcy G. W., Tinney C. G., Wright J. T., 2005, *ApJ*, 635, 1281
- Kurucz R. L., , 1998, <http://kurucz.harvard.edu/grids.html>
- Lèbre A., de Laverny P., De Medeiros J. R., Charbonnel C., da Silva L., 1999, *A&A*, 345, 936
- Maeder A., 1975, *A&A*, 43, 61
- Maeder A., Meynet G., 2000, *ARA&A*, 38, 143
- Maeder A., Zahn J.-P., 1998, *A&A*, 334, 1000
- Martić M., Lebrun J.-C., Appourchaux T., Korzenik S. G., 2004, *A&A*, 418, 295
- Mathis S., Palacios A., Zahn J.-P., 2004, *A&A*, 425, 243
- Michaud G., Richard O., Richer J., VandenBerg D. A., 2004, *ApJ*, 606, 452
- Miglio A., Montalbán J., 2005, *A&A*, 441, 615
- Morel P., Berthomieu G., Provost J., Thévenin F., 2001, *A&A*, 379, 245
- Noels A., Montalbán J., Maceroni C., 2004, in *IAU Symposium A-type stars: evolution, rotation and binarity*. pp 47–57
- Nordström B., Mayor M., Andersen J., Holmberg J., Pont F., Jørgensen B. R., Olsen E. H., Udry S., Mowlavi N., 2004, *A&A*, 418, 989
- Osaki J., 1975, *PASJ*, 27, 237
- Popielski B. L., Dziembowski W. A., 2005, *Acta Astronomica*, 55, 177
- Ribas I., Jordi C., Giménez Á., 2000, *MNRAS*, 318, L55
- Richard ., 2005, in *Element stratification in Stars: 40 years of atomic diffusion*, *EAS Publications Series Vol. 17, Evolutionary stellar models including diffusion and radiative accelerations*. pp 43–52
- Richard O., Michaud G., Richer J., 2001, *ApJ*, 558, 377
- Rogers F. J., Nayfonov A., 2002, *ApJ*, 576, 1064
- Roxburgh I. W., Vorontsov S. V., 2003, *A&A*, 411, 215
- Salpeter E. E., 1954, *Australian Journal of Physics*, 7, 373
- Samadi R., Goupil M.-J., Alecian E., Baudin F., Georgobiani D., Trampedach R., Stein R., Nordlund Å., 2005, *JApA*, 26, 171
- Théado S., Vauclair S., Castro M., Charpinet S., Dolez N., 2005, *A&A*, 437, 553
- Thoul A. A., Bahcall J. N., Loeb A., 1994, *ApJ*, 421, 828
- Tomkin J., Fekel F. C., 2006, *AJ*, 131, 2652
- VandenBerg D. A., Bergbusch P. A., Dowler P. D., 2006, *ApJS*, 162, 375
- VandenBerg D. A., Stetson P. B., 2004, *PASP*, 116, 997
- Ventura P., D'Antona F., 2005, *A&A*, 431, 279
- Ventura P., Zeppieri A., Mazzitelli I., D'Antona F., 1998, *A&A*, 334, 953
- Xiong D. R., 1985, *A&A*, 150, 133
- Young P. A., Arnett D., 2005, *ApJ*, 618, 908